International Journal of Innovative Engineering Applications

Journal homepage: https://dergipark.org.tr/ijiea

A COMPARATIVE AERODYNAMIC ANALYSIS OF NACA AND NREL AEROFOILS FOR DARRIEUS TURBINES USING CFD

Yunus Celik*[*1]

[1]*Department of Mechanical Engineering, Faculty of Engineering, Hakkari University, Turkey*

Abstract

Original scientific paper

The selection of the aerofoil plays a crucial role in achieving optimum power output, especially for the inherently low-efficient turbines, such as the Darrieus wind turbine. For this purpose, different aerofoils belonging to NACA and NREL families have been investigated in terms of the aerodynamic performance, comparatively. Although NREL aerofoils are mainly utilised for the Horizontal Axis Wind Turbines, in the present study, their effect on the Darrieus type Vertical Axis Wind Turbine has been examined. In this point of view, the influence of the various aerofoils and their thickness on the turbine performance in different operating ranges have been evaluated using Computational Fluid Dynamics (CFD). Furthermore, by considering the low and high tip speed ratios, the instantaneous blade torque coefficient, and the contours of the pressure coefficient for the selected aerofoils have been analysed to provide further understanding. The research findings show that the conventional aerofoils, such as NACA0015 and NACA0021, illustrate better power output at optimum and high tip speed ratios, while the NREL aerofoils, such as S814 and S825, are able to increase the torque generation at the relatively low tip speed ratio regions. Even though this situation makes the NREL aerofoil more desirable to design a self-starting Darrieus turbine, NREL aerofoils lost their advantages due to the higher efficiency loss at the higher tip speed ratios. In addition to this, the thicker aerofoils, such as NACA0021 and S814, yield more power output at the low tip speed ratio compared to their counterpart profiles as a result of the high pressure difference achieved between their suction and pressure sides.

Keywords: *Darrieus turbine, NACA aerofoil, NREL aerofoil, computational fluid dynamics.*

1 Introduction

As a result of the increase in energy demand, renewable energy systems have been gaining more attention compared to the past. For this reason, various types of renewable energy systems, including wind, solar, hydropower, etc., have been utilized in the production of clean energy in recent years. Among these systems, the wind energy is gaining more popularity due to its sustainability [1]. Wind energy is generally exploited using wind turbines, which are mainly classified as either Horizontal Axis Wind Turbines (HAWTs) or Vertical Axis Wind Turbines (VAWTs). Despite the fact that HAWTs dominated the wind energy sector, recent studies have focused on VAWTs due to their inherent advantages, such as cheap maintenance, no yaw mechanism required, easy fabrication, etc. [2]. The most preferred VAWT type is Darrieus turbines, this is because of the straight-blade design and higher performance output compared to the other types of VAWTs. In order to enhance the performance output of the Darrieus wind turbines, particularly at low tip speed ratios, numerous studies have attempted to optimise various types of design parameters [3]. Among the design parameters, types of aerofoils employed in the Darrieus turbines, which significantly affect the performance, have been examined in a great number of experimental and numerical studies.

The NACA aerofoil profiles have been commonly utilized in the early investigations of the Darrieus type of VAWTs. The available data that covers a wide range of the conditions for these aerofoil profiles assists in the well understanding of their aerodynamic characteristics. An experimental investigation has been carried out by Elkhoury et al. [4] to examine the performance of the different NACA aerofoils, such as NACA0018, NACA0021, and NACA634221. The findings illustrate that the NACA0018 has been found to be superior performance for the VAWT applications. Masson et al. [5] demonstrated that for the 17m Sandia VAWT, the SAND0015/47 could only improve the performance slightly at high tip speed ratios compared with the NACA0015 baseline. The static lift and drag coefficients illustrated that the SAND0015/47 was the better at low angles of attack; however, the NACA0012 aerofoil showed better performance at a high angle of attack due to the early stall of the SAND0015/47. El-Samanoudy et al. [6] investigated different aerofoils, including symmetrical and asymmetrical aerofoils, employed in the H-type VAWTs, and it has been found that the symmetrical aerofoil NACA0024 is able to produce

* Corresponding author

E-mail address: yunuscelik@hakkari.edu.tr (Y. Celik)

Received 18 February 2022; Received in revised form 11 April 2022; Accepted 09 May 2022

Doi: https://doi.org/10.46460/ijiea.1075684

higher power output compared to the asymmetrical aerofoils NACA4420 and NACA4520.

On the other hand, S-series aerofoils belonging to the NREL aerofoil families, such as S814, S815, S825, and S826 are generally used in HAWTs, therefore, a limited number of studies have been encountered in the literature for the VAWT applications. Mohamed et al. [7] has numerically examined various numbers of symmetrical and asymmetrical aerofoils, which are including the series of NACA, S-series, A-series, and FX-series. S815 aerofoil achieved a Cp value with an increase of 26.83% when compared to the symmetrical NACA aerofoils. Sengupta et al. [8] has also investigated the contribution of the blade camber and curvature signatures in terms of the performance enhancement of the VAWT having asymmetrical aerofoils, including EN0005 and S815. The aerodynamic performance of S815 aerofoil has been found to be superior to that of EN0005 aerofoil.

According to the above literature review concerning the aerofoil profile of Darrieus type VAWTs, it can be concluded that even though symmetrical NACA00XX aerofoils are commonly used for numerical and experimental investigations, asymmetrical aerofoils, such as NREL aerofoils may also be employed due to their potential to increase the torque generation at the low tip speed ratios for Darrieus type VAWTs. For this purpose, the widely employed NREL aerofoils for the HAWTs, such as S814 and S825, have been selected in order to examine their aerodynamic performances in comparison with NACA aerofoils, such as NACA0015 and NACA0021. The present study will not only be carried out for the aerodynamic performance comparison of the different aerofoils belonging NACA and NREL families on the Darrieus turbine performance but also examine the effect of the thickness of the selected aerofoils considering both low and high tip speed ratios. Moreover, the flow characteristics in terms of the contours of pressure coefficient at the vicinity of the turbine blades at the various complete revolutions will also be analyzed to provide a more comprehensive understanding.

2 Numerical Modelling

The impact of the NACA and NREL aerofoils having different thicknesses on the performance of the Darrieus wind turbine considering low and high tip speed ratios have been analysed using the Computational Fluid Dynamics (CFD) method. The CFD method is one of the most popular research tools that has been employed in the numerical studies by the researchers for not only the investigations of the wind turbine aerodynamics but also for different purposes, such as in many fluid and heat transfer studies [9][10][11].

Since the main aim of the present study is to obtain the accurate power coefficients (Cp) to compare the performance of the aerofoils for the Darrieus wind turbine applications, obtaining an accurate CFD modelling is the crucial part of the numerical simulations. For this reason, the details of the present CFD model have been given in the following sub-sections, then the final CFD model that has been used for future analyses has been compared with the published experimental and numerical data in order to observe its reliability.

2.1 Model Geometry and Computational Settings

The turbine used as a reference in the present study was chosen according to experimental study conducted by Castelli et al. [12]. The geometrical specifications and operating conditions are given in Table 1.

Table 1. The main geometrical specifications of the turbine.

Name	Value	Unit
Blade type	NACA0021	-
Blade number	3	-
Rotor Radius (R)	0.515	m
Chord length (c)	0.0858	m
Wind speed (V_∞)	9	m/s

SIMPLE algorithm for pressure-velocity coupling has been employed in the present study. The 2D transient flow has been conducted to take into account the physics of the rotational effects of the turbine by employing the Sliding Mesh Method. Furthermore, in order to ensure that the solutions were converged, two main convergence criteria have been considered to obtain accurate results. The first one is depending on the residuals, which must be lower than 10^{-5} for every time step. On the other hand, the second one is depending on the torque coefficient (Ct) which must be a difference of less than 1% between successive two complete revolutions. For this reason, every simulation has been run 20 complete revolutions in order to achieve convergence criteria. Power coefficients have been calculated by averaging the results of the last revolution.

Since the selection of the turbulence model is another important part of the numerical simulations of the Darrieus turbines, an extensive critical literature review has been carried out. It has been found that two-equation turbulence models, namely Realizable $k-\varepsilon$ and SST $k-\omega$ are the turbulence models that are commonly employed [13]. The Realizable $k-\varepsilon$ model is an improvement over the standard $k-\varepsilon$ model. In this model, new formulations for the dissipation rate and new eddy viscosity are introduced to the standard $k-\varepsilon$ model and this makes the model more consistent with the turbulent flow physics, and hence the name realizable [14]. On the other hand, the SST $k-\omega$ turbulence model was introduced, which combines the $k-\omega$ and $k-\varepsilon$ models to form a hybrid model and it becomes more popular than the standard $k-\omega$ model [15]. The $k-\omega$ model is employed for the near wall region and the $k-\varepsilon$ is used away from the wall. In order to assess the applicability of these two turbulence models for the Darrieus wind turbine simulations, these turbulence models have been used in the current research for the CFD model verification studies and compared with the experimental data.

2.2 CFD Model Verification and Validation

The computational domain has been divided into two zones, namely the rotating domain and the stationary domain. To ensure that the flow field remains continuous between the zones, interface conditions has been used to contact these two zones. The constant freestream velocity, which is perpendicular to the inlet, is defined as $V_\infty =$

$9m/s$ based on the experimental data [12]. In order to choose the appropriate domain size in terms of the high computational accuracy and low computational cost, an independency study for the domain size was conducted using three different domain sizes and the results were compared each other considering the instantaneous blade torque coefficient at the optimum tip speed ratio of 2.65, where the turbine produces the higher power coefficient. The domain sizes investigated has been provided in Table 2.

Table 2. Computation domains considered for validation study.

Domain Size	Vertical side	Horizontal side
Domain 1	32R	48R
Domain 2	64R	96R
Domain 3	128R	192R

Figure 1 illustrates the effect of the different domain sizes on the instantaneous blade torque coefficient versus the azimuthal angle. The results indicate that Domain 1 has been found to be fairly large for the computational domain since there is no significant difference obtained between other computational sizes. Therefore, Domain 1 will be employed in future studies for reducing the computational cost. The final computational domain having the values has been illustrated in Figure 2.

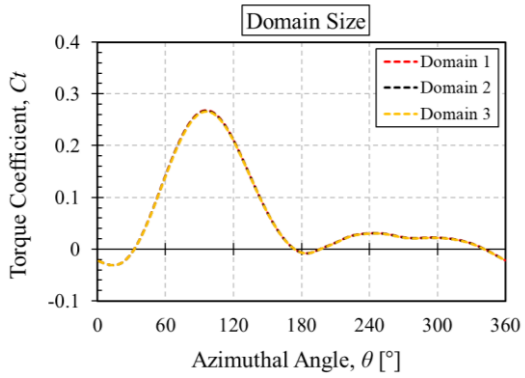

Figure 1. Effect of the different domain sizes on accuracy of the numerical solution at λ=2.65.

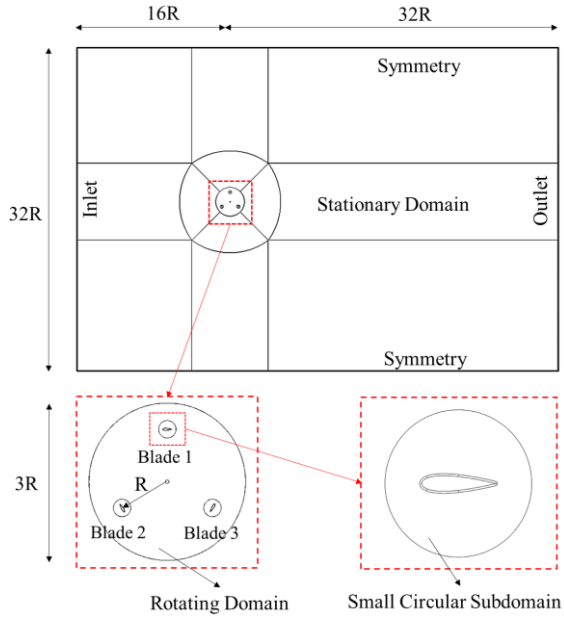

Figure 2. Computational domain and boundary conditions.

On the other hand, the meshing strategy is another important factor that affects the numerical results. Therefore, the computational domain has been meshed using the hybrid mesh technique, as shown in Figure 3, due to the fact that it is the most appropriate mesh type for reducing the total mesh element number of the computational domain [16]. In the current investigation, 25 mesh layers with the first cell height of about 2.5×10^{-5}m has been used to achieve a maximum non-dimensional wall distance y^+ value of 2.25 and average $y^+ < 1$. Thus, the appropriate calculation of the aerodynamic forces in the boundary layer can be obtained by preserving these values [17].

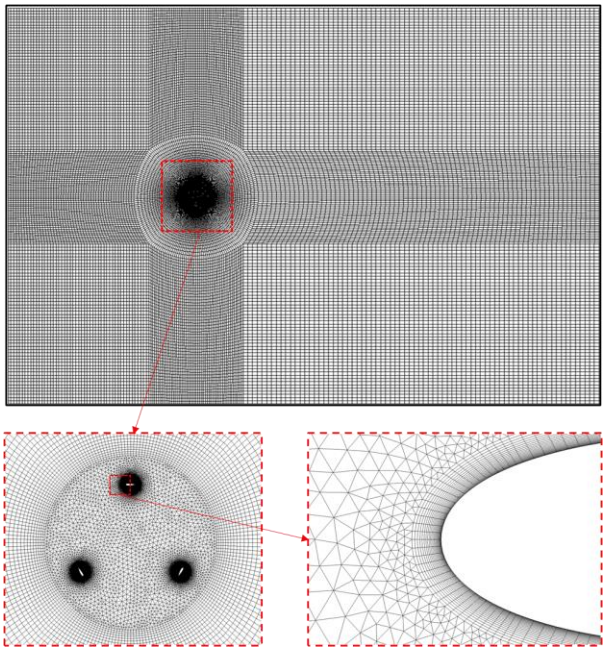

Figure 3. Mesh distribution for whole computational domain, rotating domain, and leading edge of aerofoil.

A mesh independency study was also carried out to achieve the final mesh that is not affected by changing the mesh number in both the around the aerofoil and the whole computational domain. For this purpose, four different mesh sizes were created by use of the ANSYS Meshing Module and compared to each other by using the instantaneous blade torque coefficient. The number of mesh around the aerofoil and its corresponding mesh number in the computational domain are given in Table 3.

Table 3. Mesh sizes considered for validation study.

Mesh Size	Number of Nodes around aerofoil	Total Mesh number
Mesh 1	90	64320
Mesh 2	180	122508
Mesh 3	400	240640
Mesh 4	1000	525681

Figure 4 demonstrates a plot of the comparison of the torque coefficients versus blade azimuthal angle for various mesh sizes at a tip speed ratio of 2.65. Mesh 3 and 4 have a small difference in torque coefficients throughout all azimuthal angles, as seen in the figure, however, Mesh 1 and Mesh 2 are quite different. As a consequence, the most reasonably accurate and computationally efficient number of nodes around the aerofoil have been

determined to be 400, which is corresponding to around 240640 number of mesh in whole domain, and selected for the further simulations of the Darrieus wind turbine in the present study.

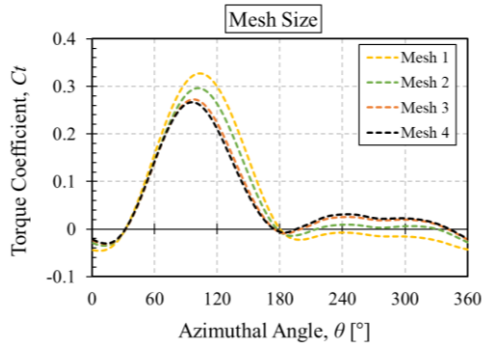

Figure 4. Effect of the different mesh sizes on accuracy of the numerical solution at λ=2.65.

Furthermore, as shown in Table 4, three time steps, which are $\Delta t1$ =0.000753748s, $\Delta t2$ =0.000376874s, and $\Delta t3$ =0.000188437s, have been selected to examine the influence of the length of time steps on the results at the tip speed ratio of 2.65. The selected time step sizes are corresponding to 2°, 1.5°, and 1°, respectively. The results, as shown in Figure 5, reveal that there is only a small variation observed between Δt2 and Δt3 with the similar trend in the torque coefficient. Thus, to lower the processing time, $\Delta t2$ =0.000376874s is chosen for further simulations.

Table 4. Time step sizes considered for validation study.

Time Step Size	Degree (°)	Second (s)
Time Step 1	2°	0.000753748
Time Step 2	1°	0.000376874
Time Step 3	0.5°	0.000188437

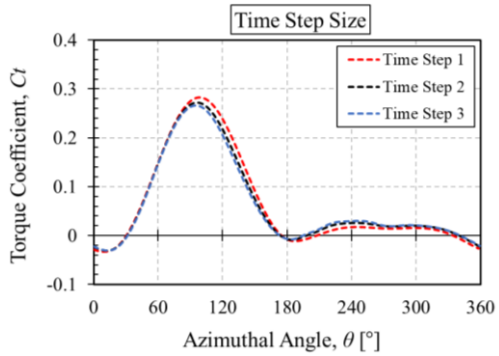

Figure 5. Effect of the different time step sizes on accuracy of the numerical solution at λ=2.65.

The current CFD model, which uses both Realizable $k-\varepsilon$ and SST $k-\omega$ turbulence models, is compared to experimental and numerical data acquired by Castelli et al. [12] and results are illustrated in Figure 6. As shown in the figure, the present CFD model with SST $k-\omega$ turbulence model is capable of accurately predicting turbine performance, especially in the low tip speed ratio regions. Due to these close results achieved from present CFD model compared to author's numerical results, the present model with SST $k-\omega$ turbulence model can be considered as a reasonable model for predicting the Darrieus turbine performance.

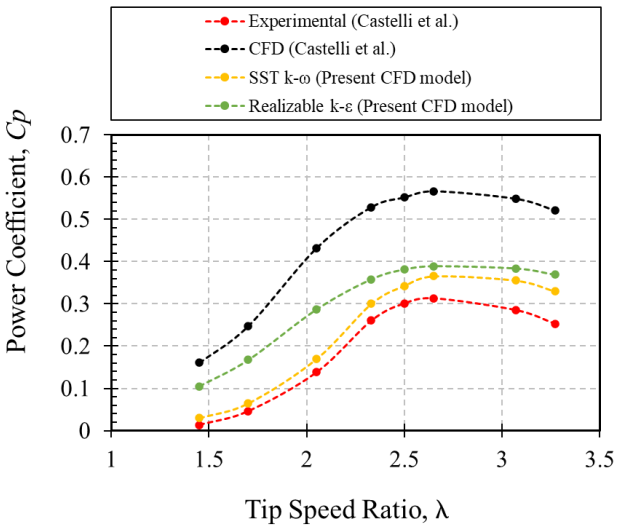

Figure 6. The present CFD model comparison with the experimental and numerical results of Castelli et al. [12].

3 Research Findings and Discussions

The power output of the Darrieus wind turbines is generally depending on several important parameters, such as aerofoil profile, solidity, wind speeds, etc. The aim of the present research is to determine how different aerofoil designs impact the ability of the turbine to produce power at varied tip speed ratios. The tip speed ratio range has been determined according to the tip speed ratios tested in the experimental study [12]. For this reason, aerofoils belonging NACA and NREL aerofoil families, namely NACA0015, NACA0021, S814, and S825, have been selected for the present investigation. The schematic of the selected aerofoils is illustrated in Figure 7. NACA0015 and S825 are thin aerofoils while NACA0021 and S814 are relatively thick aerofoils.

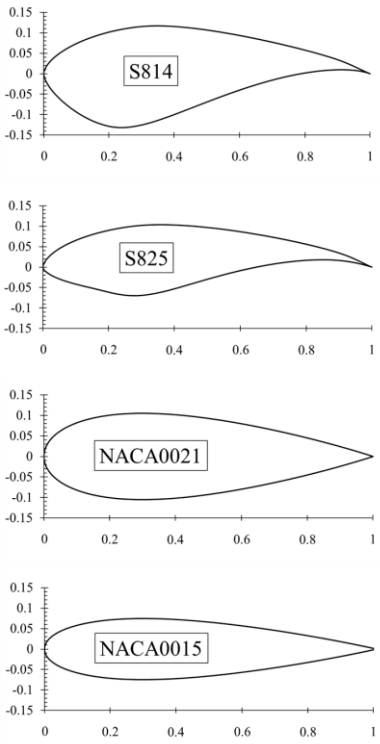

Figure 7. Investigated aerofoil profiles.

The current study considers a typical operating range of small-scale Darrieus wind turbines: a tip speed ratio varying between 1.45 and 3.27. The reason of selection of the low value of tip speed ratio, such as λ=1.45, is to assess the self-starting ability of the turbine having different aerofoil profiles. On the other hand, high tip speed ratios, such as λ=3.27, assist to further understanding of the effect of the aerofoil profiles on the power output at such high tip speed ratios.

Figure 8 illustrates the power coefficients as a function of the tip speed ratio for the Darrieus wind turbines having different aerofoil profiles. As can be observed in the figure, different aerofoil profiles can cause different effects on the turbine performance at different operating conditions. For instance, when compared the aerofoil from the same families, the thin aerofoils, such as NACA0015 and S825 produce higher power output at the higher tip speed ratio of 3.7, while the thick aerofoils, such as NACA0021 and S814 are able to produce higher power output at the lower tip speed ratio of 1.45.

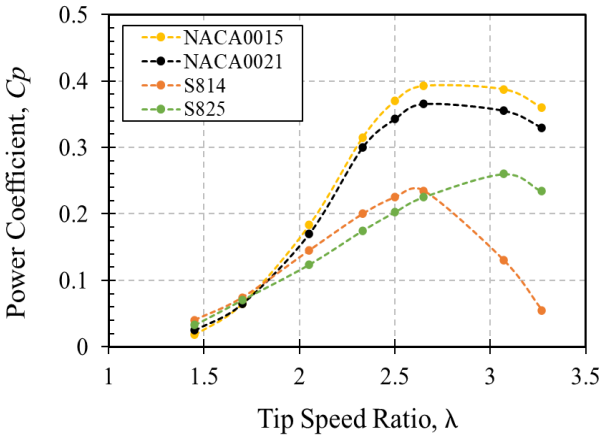

Figure 8. The effect of the aerofoil profile on the power coefficient of the Darrieus turbine at different tip speed ratios.

Furthermore, Figure 9 shows the enlarged view of the Figure 8 with more focus on the lower tip speed ratio regions. The reason behind the illustration of the enlarged view of the power coefficient as a function of the tip speed ratio curve is to provide a much closer view of the low tip speed ratio region, which assists in the understanding of the influence of aerofoil types on the turbine self-starting capability. It is observed that although the turbine performance increases with the increase in the aerofoil thickness at the lower tip speed ratio regions, NREL aerofoil families produce more power output compared to the NACA aerofoils. This situation can lead to increase the self-starting ability and these aerofoils can be preferred for the small-scale Darrieus wind turbines owing self-starting deficiency. However, due to the higher efficiency loss at the optimum and higher tip speed ratio values, NREL aerofoils can lose their advantages. Therefore, depending on the purpose, the optimum aerofoil type should be selected.

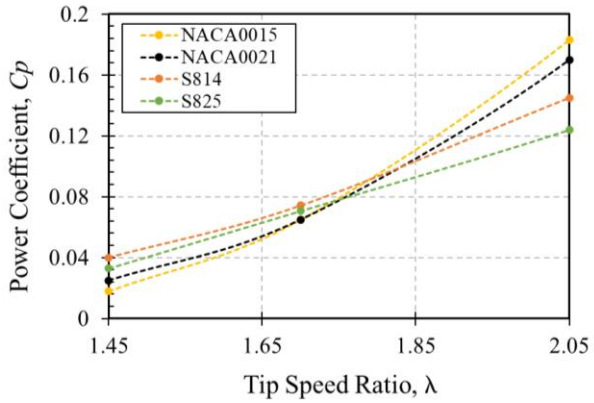

Figure 9. Enlarged view of power coefficient/tip speed ratio curve.

Moreover, the contours of the pressure coefficient have been analysed at the low and high tip speed ratios in order to understand the behaviour of the turbine in contact with the wind and indicate the reason for the power efficiency obtained by applying different NACA and NREL aerofoils. To simplify the analysis, only two tip speed ratios, namely λ=1.45 and λ=3.27 have been considered since the turbines investigated indicated different performance at selected tip speed ratios. In addition to the pressure contours, the variation of instantaneous torque versus azimuthal angles for the aerofoils at both tip speed ratios was also examined. Figure 10 illustrates a plot of the instantaneous blade torque coefficients versus the azimuthal angle for the aerofoils investigated. In the upstream part of the turbine, where the azimuthal angle (θ) varies between 0° and 180°, the NREL aerofoils illustrates better aerodynamic performance compared to the NACA aerofoils. In addition to this, the thicker NREL aerofoil, which is S814, produces higher torque coefficient when compared to thin S825 aerofoil. This situation can be also observed in Figure 11, where the contours of the pressure coefficients are illustrated. The pressure difference between the suction and pressure sides of the S814 aerofoil is higher than the S825, and this causes a higher torque generation. In contrast, when the performance of the aerofoils assessed in the downstream part of the turbine, where the azimuthal angle (θ) varies between 180° and 360°, since there is no significant difference observed between the suction and pressure sides, an about similar value of the torque coefficients has been obtained.

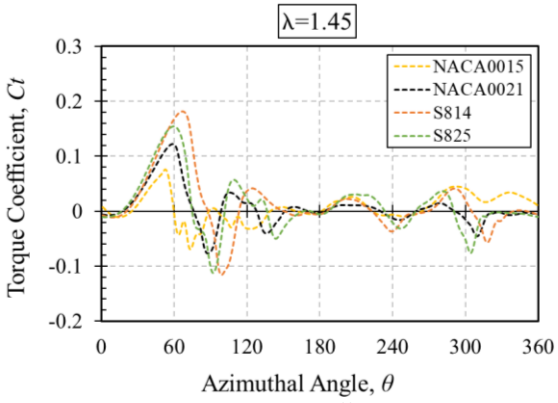

Figure 10. Instantaneous blade torque coefficient versus the azimuthal angle for aerofoils investigated at λ=1.45.

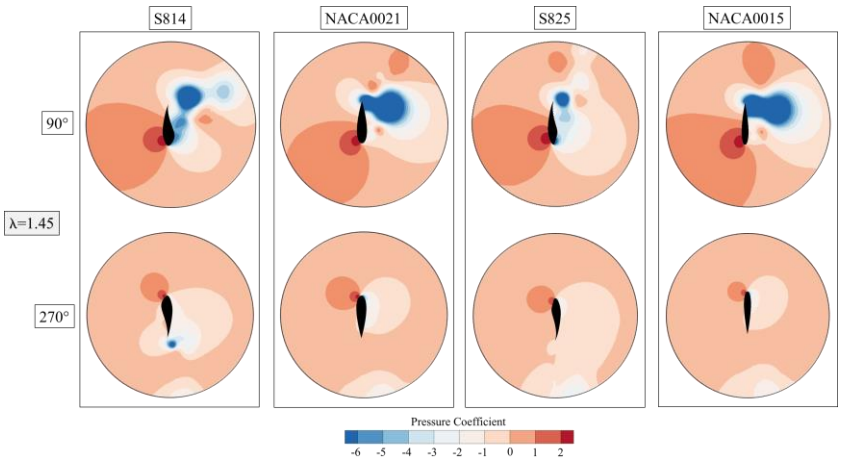

Figure 11. The contours of pressure coefficient at the tip speed ratio of 1.45 for the aerofoils investigated considering azimuthal angle of 90° and 270°

Furthermore, the change in the instantaneous blade torque coefficient versus the azimuthal angle has been also examined for the aerofoils at λ=3.27 (see Figure 12). On the contrary of the λ=1.45, the better performance can be achieved in the upstream part of the turbine when the NACA aerofoil families are employed at λ=3.27, as seen in the figure. However, while the thin aerofoil NACA0015 produces a higher torque generation in the upstream part of the turbine, NREL aerofoils are able produce a higher torque coefficient in the downstream part of the turbine. This situation can be clearly observed in the contours of the pressure figures illustrated in Figure 13. The higher pressure difference between the suction and pressure sides of the NACA0015 than that of other aerofoils leads to higher torque generation in the upstream part of the turbine. Additionally, when the downstream part of the turbine is considered, since the pressure difference between the suction and pressure sides of S825 is much obviously higher at the θ=270° compared to the other aerofoils, the instantaneous torque coefficient of S825 is higher.

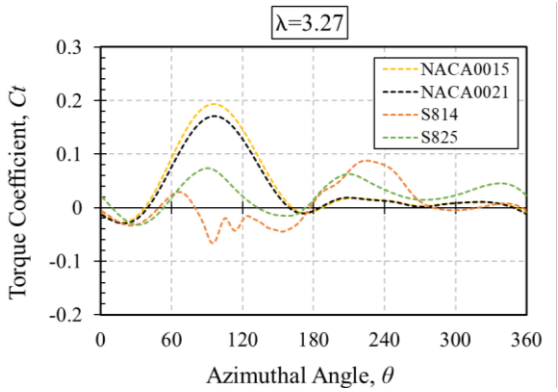

Figure 12. Instantaneous blade torque coefficient versus the azimuthal angle for aerofoils investigated at λ=3.27.

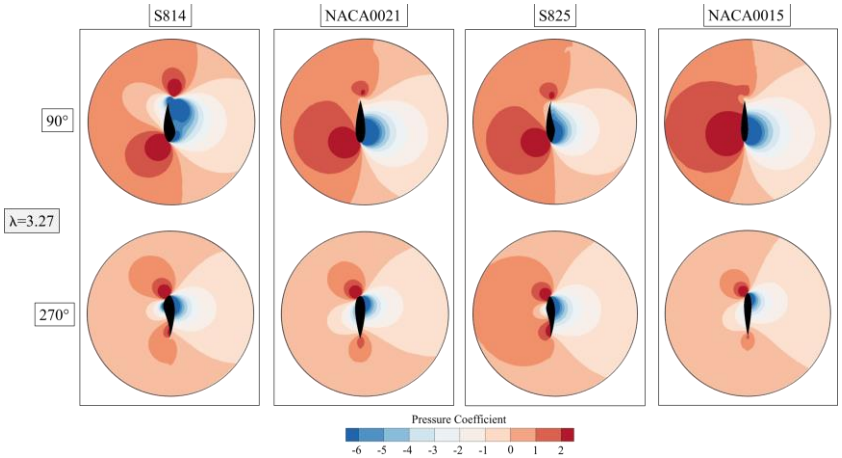

Figure 13. The contours of pressure coefficient at the tip speed ratio of 3.27 for the aerofoils investigated considering azimuthal angle of 90° and 270.

4 Conclusion

The present CFD model, which was extensively validated with the experimental and numerical results, has been employed to investigate the impact of the various aerofoil profiles belonging to the NACA and NREL families on the power performance of the Darrieus wind turbine considering the low and high operating ranges. The aerofoils investigated, namely NACA0015, NACA0021, S814, and S825, have been selected by considering having a different thickness. The results obtained in the present study show that NACA aerofoils are more advantageous at high λ values while NREL aerofoil can be utilized due to higher power output at relatively low λ values, which may assist turbine self-starting ability. Furthermore, the thicker aerofoils, such as NACA0021 and S814, produce a higher power output at λ=1.45 compared to their counterpart profiles. On the other hand, at λ=3.27, the thinner aerofoils, such as NACA0015 and S825, are able to produce more power output. Consequently, NACA aerofoils can be still

preferable due to their advantages of the higher torque output at high λ values, but NREL aerofoils are surprisingly producing more power at lower λ values, which makes them more desirable to overcome the self-starting issue of the Darrieus wind turbine.

Declaration of Competing Interest

The authors declare that they have no known competing financial interests or personal relationships that could have appeared to influence the work reported in this paper. Ethics committee approval is not required.

References

[1] Kaya, M. N., Kose, F., Ingham, D., Ma, L., & Pourkashanian, M. (2018). Aerodynamic performance of a horizontal axis wind turbine with forward and backward swept blades. *Journal of Wind Engineering and Industrial Aerodynamics*, 176, 166-173.

[2] Celik, Y., Ma, L., Ingham, D., & Pourkashanian, M. (2020). Aerodynamic investigation of the start-up process of H-type vertical axis wind turbines using CFD. *Journal of Wind Engineering and Industrial Aerodynamics*, 204, 104252.

[3] Celik, Y. (2021). *Aerodynamics and Self-Starting of Vertical Axis Wind Turbines with J-Shaped Aerofoils* (Doctoral dissertation, University of Sheffield).

[4] Elkhoury, M., Kiwata, T., & Aoun, E. (2015). Experimental and numerical investigation of a three-dimensional vertical-axis wind turbine with variable-pitch. *Journal of wind engineering and Industrial aerodynamics*, 139, 111-123.

[5] Masson, C., Leclerc, C., & Paraschivoiu, I. (1998). Appropriate dynamic-stall models for performance predictions of VAWTs with NLF blades. *International Journal of Rotating Machinery*, 4(2), 129-139.

[6] El-Samanoudy, M., Ghorab, A. A. E., & Youssef, S. Z. (2010). Effect of some design parameters on the performance of a Giromill vertical axis wind turbine. *Ain Shams Engineering Journal*, 1(1), 85-95.

[7] Mohamed, M. H. (2012). Performance investigation of H-rotor Darrieus turbine with new airfoil shapes. *Energy*, 47(1), 522-530.

[8] Sengupta, A. R., Biswas, A., & Gupta, R. (2016). Studies of some high solidity symmetrical and unsymmetrical blade H-Darrieus rotors with respect to starting characteristics, dynamic performances and flow physics in low wind streams. *Renewable Energy*, 93, 536-547.

[9] Yadav, A. S., Shukla, O. P., Sharma, A., & Khan, I. A. (2022). CFD analysis of heat transfer performance of ribbed solar air heater. *Materials Today:* Proceedings.

[10] Zhao, Y., Akolekar, H. D., Weatheritt, J., Michelassi, V., & Sandberg, R. D. (2020). RANS turbulence model development using CFD-driven machine learning. *Journal of Computational Physics*, 411, 109413.

[11] Lye, K. O., Mishra, S., & Ray, D. (2020). Deep learning observables in computational fluid dynamics. Journal of *Computational Physics*, *410*, 109339.

[12] Castelli, M. R., Englaro, A., & Benini, E. (2011). The Darrieus wind turbine: Proposal for a new performance prediction model based on CFD. *Energy*, 36(8), 4919-4934.

[13] Song, C., Zheng, Y., Zhao, Z., Zhang, Y., Li, C., & Jiang, H. (2015). Investigation of meshing strategies and turbulence models of computational fluid dynamics simulations of vertical axis wind turbines. *Journal of Renewable and Sustainable Energy*, 7(3), 033111.

[14] Pouraria, H., & Park, W. G. (2010, September). Comparison of different two equation turbulence models for studying the effect of cold outlet diameter on cooling performance of vortex tube. In *2010 International Conference on Mechanical and Electrical Technology* (pp. 304-308). IEEE.

[15] Celik, Y., Ingham, D., Ma, L., & Pourkashanian, M. (2022). Design and aerodynamic performance analyses of the self-starting H-type VAWT having J-shaped aerofoils considering various design parameters using CFD. *Energy*, 251, 123881.

[16] Almohammadi, K. M., Ingham, D. B., Ma, L., & Pourkashan, M. (2013). Computational fluid dynamics (CFD) mesh independency techniques for a straight blade vertical axis wind turbine. *Energy*, 58, 483-493.

[17] Elsakka, M. M., Ingham, D. B., Ma, L., & Pourkashanian, M. (2019). CFD analysis of the angle of attack for a vertical axis wind turbine blade. *Energy Conversion and Management*, 182, 154-165.